Semi-Annual Status Report

"The Absolute Radiometric Calibration of the Advanced Very High Resolution Radiometer"

P. N. Slater

P. M. Teillet

Y. Mao

Optical Sciences Center
University of Arizona
Tucson Arizona 85721

September 1987

1. Introduction

An increasing number of remote sensing investigations require radiometrically calibrated imagery from the NOAA AVHRR sensors. Although a pre-launch calibration was done, there is no capability for monitoring any changes in calibration in-orbit for the visible and near infrared spectral bands. Hence, the possibility of using the reflectance-based method developed at White Sands for in-orbit calibration of Landsat TM data (Slater et al., 1987) to calibrate the AVHRR sensor has been under investigation.

The purpose of this document is to provide a status report on research activities under NASA grant NAG 5-859. Section 2 describes the methodology and presents early results obtained for the NOAA-9 AVHRR. Section 3 summarizes the current status and plans for future activities.

Those involved in the preparation of this report were P. M. Teillet[1], Yalan Mao and P. N. Slater. Yi Ding helped with the data reduction. Others involved in data collection at White Sands and Edwards Air Force Base, partially in support of this activity, are R. J. Bartell, S. F. Biggar and R. P. Santer from the Optical Sciences Center and R. D. Jackson and M. S. Moran from the USDA Water Conservation Laboratory in Phoenix.

2.0 Methodology and Early Results for NOAA-9 AVHRR

The reflectance-based approach to radiometric calibration at White Sands is strongly dependent on the accurate characterization of ground reflectance (among other things) at the time of satellite overpass. Suitable reflectance-factor measurements have been made over terrain areas corresponding to numerous Landsat TM or SPOT HRV pixels (Slater et al., 1987; Jackson et al., 1987). However, this

---

[1]P. M. Teillet is visiting the University of Arizona on a one-year leave of absence from the Canada Centre for Remote Sensing.

approach becomes impractical for the calibration of NOAA AVHRR image data with pixel dimensions of 1.1 km by 1.1 km or greater. One alternative is to acquire AVHRR and TM imagery on the same day and take advantage of the detailed TM calibration results to effect a calibration of the AVHRR sensor.

On August 28, 1985, ground reflectance-factor measurements in TM bands, and atmospheric data were collected at Chuck Site, White Sands, New Mexico. The methodology and results for reflectance-based calibrations of the Landsat-5 TM on this date and four others have been presented elsewhere (Slater et al., 1986). These show a ± 2.8% uncertainty in precision (1σ RMS standard deviation) for the six solar-reflective bands over the five dates. Table 1 lists the results for August 28, 1985. The TM band 4 values differ slightly from those reported previously (Slater et al., 1986) because of a refinement in the way water-vapor absorption is handled.

Given the calibration of TM bands 3 and 4 and NOAA-9 AVHRR imagery in bands 1 and 2 on the same day, the prediction of radiance at the AVHRR sensor may be divided into four steps:

(i) determination of ground reflectance (using TM bands 3 and 4) averaged over as large an AVHRR pixel area as possible (essentially 2 pixels by 2 lines) in the alkali flat region of White Sands;

(ii) spectral redistribution of ground reflectance into seven narrower bands encompassing AVHRR bands 1 and 2;

(iii) prediction of radiance at the AVHRR sensor in the narrower bands using measured atmospheric parameters and radiative transfer computations;

(iv) reconstitution of predicted radiances into spectral radiance values in AVHRR bands 1 and 2, and expression of the absolute radiometric calibration in terms of counts per unit radiance.

Table 1. Calibration of the Thematic Mapper at White Sands on August 28, 1985.
(*With additional gaseous transmittance due to H_2O, O_2, CO_2)

Solar zenith angle Z:	35.954	Latitude: 32 deg 55 min	
Solar distance in AU:	1.0098	Longitude: 106 deg 22 min	
Junge size distribution:	3.77	Elevation: 1196 m	
Aerosol size range: 0.02 to 5.02 μm		Pressure: 658.1 mm Hg or 877.42 mbars	
Refractive index: 1.54 - 0.01i		Temperature: 29.5 deg C	
Time of overpass: 10:08.4 MST		Relative humidity: 21%	
Calculated visibility 200 km		Nadir viewing angle: 5 deg.	

Thematic Mapper bands	3	4	4*
Central wavelength μm	0.6607	0.8382	0.8382
Tau Mie	0.0588	0.0386	0.0386
Tau Rayleigh	0.0403	0.0155	0.0155
Tau ozone	0.0141	0.0016	0.0016
Tau water vapor	0.0000	0.0341	0.0341
Tau carbon dioxide	0.0000	0.0000	0.0000
Single scattering albedo	0.8133	0.7824	0.7824
Spectral reflectance	0.6018	0.6422	0.6422
Eo across band in W/m2.μm	1545.0	1042.8	1042.8
Average image digital counts	203.31	166.14	166.14
Preflight cal gains	10.203	10.821	10.821
Preflight cal offsets	1.8850	2.2373	2.2373
IC cal gains for 28 Aug 1985	9.25	10.299	10.299
IC cal offsets for 28 Aug 1985	3.1170	2.7320	2.7320
Normalized code radiance	0.1471	0.1496	0.1538
Code TM L in W/m2.sr.μm	222.84	153.02	157.36
Spectral L from preflight cal	197.42	151.47	151.47
Spectral L from IC cal	216.42	158.66	158.66
% (Code-Pre)/Pre	12.9	1.0	3.9
% (Code-IC)/IC	3.0	-3.6	-0.8
Counts per unit radiance	0.912	1.086	1.056

****

Case for Rayleigh Atmosphere

Normalized code radiance	0.1555	0.1655
Code TM L in W/m2.sr.μm	235.57	169.28
Counts per unit radiance	0.863	0.981

****

Case for No Atmosphere

Normalized radiance	0.1551	0.1655
TM L in W/m2.sr.μm	234.90	169.20
Counts per unit radiance	0.866	0.982

****

2.1 Determination of Ground Reflectance from TM Imagery

Since the TM and AVHRR sensors acquired images with very different observation geometries (TM with near-nadir viewing in a descending orbit, AVHRR with significant off-nadir viewing in an ascending orbit), a geometric registration procedure was used to match the two images. From the superimposed images (Figures 1-4), a relatively uniform area of two by two AVHRR pixels was selected in the alkali-flat region of White Sands. The digital counts for this area and for the corresponding area in the TM imagery were extracted and averaged. The TM values are presented in Table 2, together with radiance values based on the White Sands calibration from Chuck Site (Code) and based on the TM Internal Calibrator (IC). Results are also given for an area similar in size in the dunes area at White Sands.

In order to relate the TM radiance values obtained for the AVHRR test area to ground reflectance factors, a series of atmospheric computations were carried out using the Herman radiative transfer code (Herman and Browning, 1975) and the atmospheric input parameters listed in Table 1. With ground reflectance values ranging from 0.00 to 0.99 at the input, corresponding radiance values at satellite altitude were generated by the code. For both TM bands 3 and 4, the resulting relationship between predicted radiance and ground reflectance is quite linear. These linear relationships were then used to obtain reflectance factors from the code radiance values derived from TM bands 3 and 4 for the AVHRR test area (Table 2).

Table 2. Ground reflectances for the AVHRR test area from TM imagery.

TM Band	Area	Average DC	L(IC) (W/M2.SR.μM)	L(CODE) (W/M2.SR.μM)	Reflectance	Central Wavelength
3	Alkali Flat	172.3	182.9	188.3	0.510	0.6607
3	Dunes	239.9	256.0	263.6	0.720	0.6607
4	Alkali Flat	144.2	137.3	132.4	0.555	0.8382
4	Dunes	195.6	187.2	180.5	0.760	0.8382

Figure 1. Digital counts of NOAA-9 AVHRR channel 1 at White Sands on August 28, 1985. The higher values in the upper portion correspond to the dunes area, whereas the lower values in the lower-left are in the alkali-flat region.

291	333	342	355	392	410	397	365
342	381	400	414	428	434	423	412
382	405	414	428	447	464	473	475
374	386	413	441	462	482	476	478
384	415	440	459	469	475	478	483
402	432	453	465	472	473	477	481
398	432	452	464	471	473	476	481
409	432	445	456	459	458	467	478
417	431	440	444	440	438	453	471
421	425	432	438	435	442	458	470
400	419	425	435	440	448	460	467
380	403	415	426	440	447	457	463
373	389	404	416	433	442	446	459
366	375	387	401	416	425	429	447
365	369	371	382	394	408	424	443
355	360	368	384	386	369	368	417
360	368	374	379	376	361	366	408
365	373	380	386	379	359	366	406
364	373	381	387	368	366	394	427
367	372	370	365	369	400	431	450
365	364	361	370	392	421	443	451
367	372	369	379	410	437	449	447
365	366	368	386	418	442	449	443

Figure 2. Digital Counts of NOAA-9 AVHRR channel 2 at White Sands on August 28, 1985. This higher values in the upper portion correspond to the dunes area, whereas the lower values in the lower-left are in the alkali-flat region.

279	313	323	331	357	371	360	338
318	347	361	373	384	387	376	368
349	365	371	382	398	411	417	418
339	348	369	392	408	416	419	420
347	371	390	404	412	417	420	423
361	384	399	408	413	415	418	421
357	383	397	406	412	414	417	421
366	383	392	403	403	404	411	419
371	381	388	392	390	390	400	414
373	376	382	387	386	391	403	412
357	371	375	382	388	394	404	409
341	356	366	375	386	392	401	406
335	378	358	367	380	387	392	402
330	336	345	356	366	373	377	392
326	329	331	341	350	362	374	389
319	323	329	342	345	332	331	369
324	330	336	339	337	325	331	363
329	336	341	346	339	323	332	362
327	335	342	346	328	328	354	377
329	333	331	327	331	356	380	394
327	326	322	331	349	371	388	395
329	332	331	340	363	382	392	392
327	328	332	346	368	387	392	387

Figure 3. Digital counts of Landsat-5 TM channel 3 for alkali-flat region of White Sands on August 28, 1985.

164 164 167 172 173 174 170 171 177 175 173 171 174 173 170 170

161 163 167 172 171 175 175 177 170 170 173 175 174 172 172 164

162 165 166 168 171 171 170 177 177 175 173 174 166 166 164 161

166 169 167 167 168 173 175 173 165 173 176 174 175 168 158 161

168 171 172 171 172 173 176 171 166 172 176 176 175 173 165 162

169 171 174 172 176 177 177 174 173 166 166 167 175 172 164 169

171 170 170 172 172 174 177 174 175 175 174 169 166 172 164 162

171 170 171 172 171 175 175 174 174 174 174 171 161 170 164 160

168 170 175 170 177 177 176 176 174 176 173 175 176 175 174 173

166 168 174 175 182 183 175 175 174 175 173 176 179 175 173 173

170 171 174 175 173 178 178 174 179 175 177 172 173 171 173 173

171 172 176 175 175 175 183 183 182 182 176 172 170 164 170 177

172 172 172 173 172 174 184 186 185 182 176 170 178 173 169 171

170 173 169 169 172 175 182 187 180 168 169 170 165 169 174 172

158 169 169 169 169 174 179 186 182 169 170 170 169 169 173 172

156 156 167 171 170 174 179 184 184 180 176 169 168 173 175 169

Figure 4. Digital counts of LANDSAT-5 TM channel 4 for alkali-flat reigion of White Sands on August 28, 1985.

144 143 146 147 150 157 157 153 147 151 151 140 140 151 151 143

145 145 145 147 154 154 157 153 147 146 149 147 148 154 149 148

142 145 148 149 146 146 155 150 149 151 147 147 151 146 146 141

145 146 144 152 152 146 149 153 151 155 155 149 151 138 146 145

144 147 144 144 146 146 149 157 159 159 150 154 143 138 146 144

135 141 141 145 144 144 148 157 156 156 150 141 146 138 135 135

135 126 126 141 142 148 148 158 158 151 145 145 146 150 150 146

140 140 140 145 142 144 145 145 145 156 156 153 143 141 141 146

148 145 147 144 144 152 152 152 145 153 152 152 139 139 146 149

143 129 129 140 150 145 145 141 151 153 150 154 154 141 141 141

144 129 141 140 147 147 145 141 149 153 145 141 141 140 138 145

144 137 141 145 140 140 143 144 152 143 145 137 142 135 137 137

143 139 137 145 144 137 145 147 145 132 132 145 145 135 141 147

142 145 144 144 144 146 145 148 145 145 140 145 141 132 143 146

144 146 146 146 144 146 143 143 147 147 143 145 141 136 142 142

139 143 143 144 149 146 145 141 141 149 146 139 139 136 130 129

2.2 Spectral Redistribution of Ground Reflectance

Since NOAA-9 AVHRR spectral bands 1 (0.570-0.700 μm) and 2 (0.714-0.983 μm) are not narrow bands (Figure 5) and the Herman radiative transfer code assumes monochromaticity, they were subdivided into small segments. Channel 1 was divided into three bands centered at 595, 635, and 680 nm, whereas channel 2 was divided into four bands centered at 760, 840, 900, and 960 nm. Before running the Herman code at these wavelengths, the reflectance values obtained in the previous section (2.1) were adjusted in two ways.

Firstly, at the NOAA-9 satellite overpass time of 21:27 Universal Time, the solar zenith angle was 39.85 degrees, whereas at the Landsat 5 satellite overpass time of 17:08 Universal Time, the solar zenith angle was 35.95 degrees. Moreover, the viewing nadir angle was 23.62 degrees for the AVHRR sensor and 5 degrees for the TM sensor. Thus, corrections for non-lambertian effects were applied to the TM band 3 and 4 reflectance factors on the basis of bi-directional reflectance measurements made for the gypsum surface at White Sands on March 15, 1986 (Figure 6).

Secondly, the reflectance factors derived in the previous section were for TM bands 3 and 4, but ground reflectances for input to the Herman code were required at seven other wavelengths. Fortunately, off-nadir ground reflectance measurements with a Barnes Modular Multispectral 8-channel Radiometer[2] (Robinson et al., 1979) are available for approximately the same solar zenith as that for the AVHRR overpass on August 28, 1985. Those measurements were used by Ray Jackson to derive an equation relating the surface reflectance at Chuck Site to wavelength in

---

[2]Trade names and company names are included for the convenience of the reader and imply no endorsement of the product or company by the University of Arizona or the United States Department of Agriculture.

micrometers (Table 3):

$$\rho(\lambda) = a_0 + a_1\lambda + a_2\lambda^2 + a_3\lambda^3 + a_4\lambda^4.$$

With this equation and coefficients from Table 3 for the case of 24.6 degrees nadir view angle, reflectances were calculated at the seven wavelengths of interest (Table 4). These values were also adjusted to take into account the difference in surface reflectance between Chuck Site and the alkali-flat region, the latter being darker in the spectral domain of interest. More specifically, the three reflectances in the AVHRR band-1 region were shifted downward by the difference between $\rho(\lambda = 0.6607)$ from Jackson's equation and the relevant reflectance value (0.510) from Table 2. Similarly, the four reflectances in AVHRR band-2 region were shifted downward by the difference between $\rho(\lambda = 0.8382)$ and the relevant reflectance value (0.555) from Table 2.

Table 3. Surface Reflectance as a Function of Wavelength for Different View Angles.

Date	Solar Zenith Angle (Degrees)	View Nadir Angle (Degrees)	a_0	a_1	a_2	a_3	a_4
08 Mar 86	40.10	31.2	-0.84395	6.00165	-9.18091	6.2899	-1.6215
15 Mar 86	41.01	24.6	-1.85425	10.69285	-18.28977	14.1966	-4.1502
20 Mar 86	38.62	18.4	-1.64884	9.53550	-16.16274	12.5705	-3.7022

Table 4. Reflectances for the Seven Narrower Bands Subdividing the AVHRR Bands.

Wavelength λ (μm)	Reflectance $\rho(\lambda)$ (Chuck Site)	Shift (See Text)	Reflectance (Alkali Flat)
0.595	0.5032	0.0102	0.4930
0.635	0.5210	0.0102	0.5108
0.680	0.5362	0.0102	0.5260
0.760	0.5555	0.0193	0.5362
0.840	0.5706	0.0193	0.5513
0.900	0.5810	0.0193	0.5617
0.960	0.5903	0.0193	0.5710

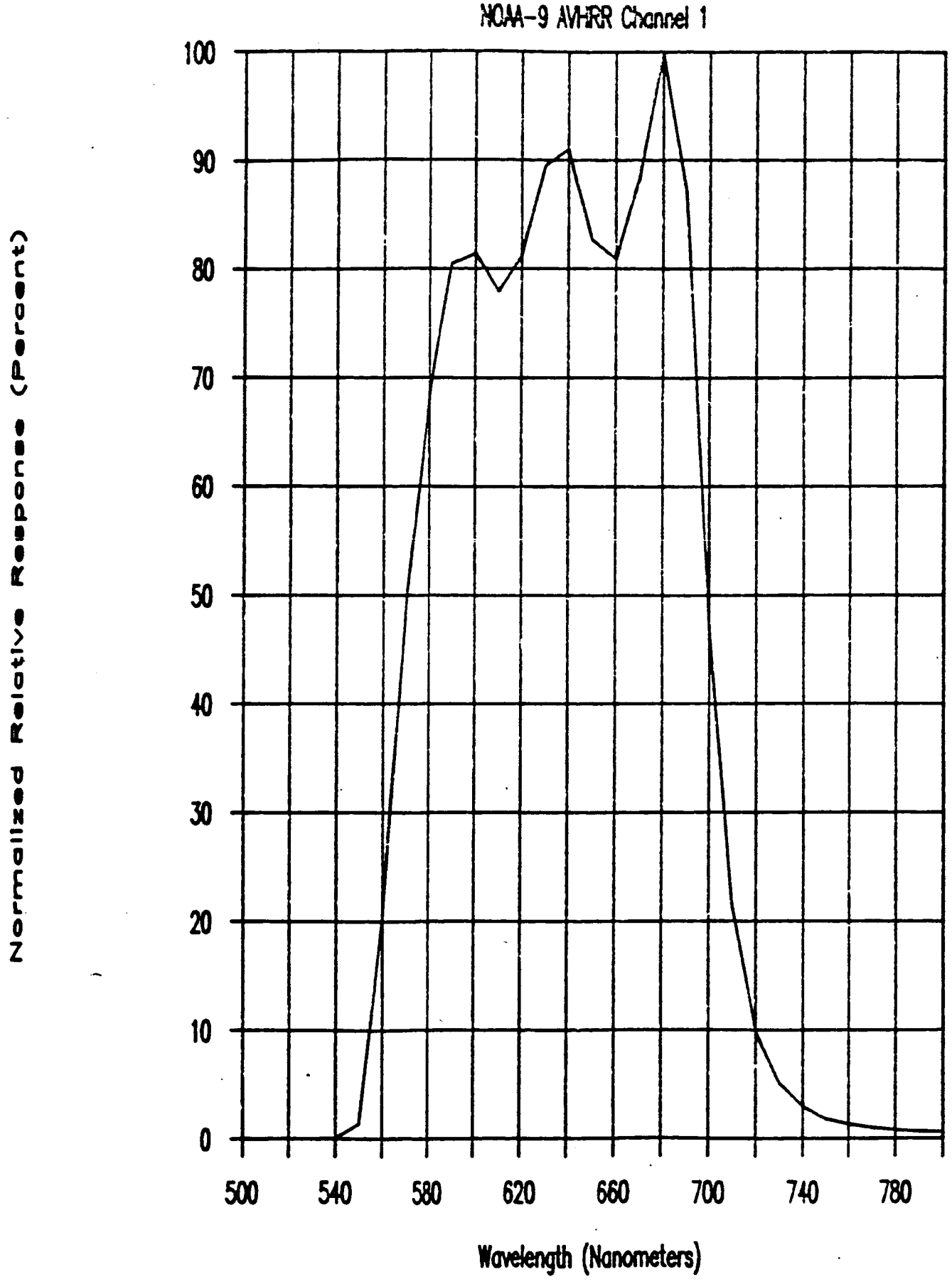

Figure 5a. Relative Spectral Response for NOAA-9 AVHRR Channel 1 (Kidwell, 1986).

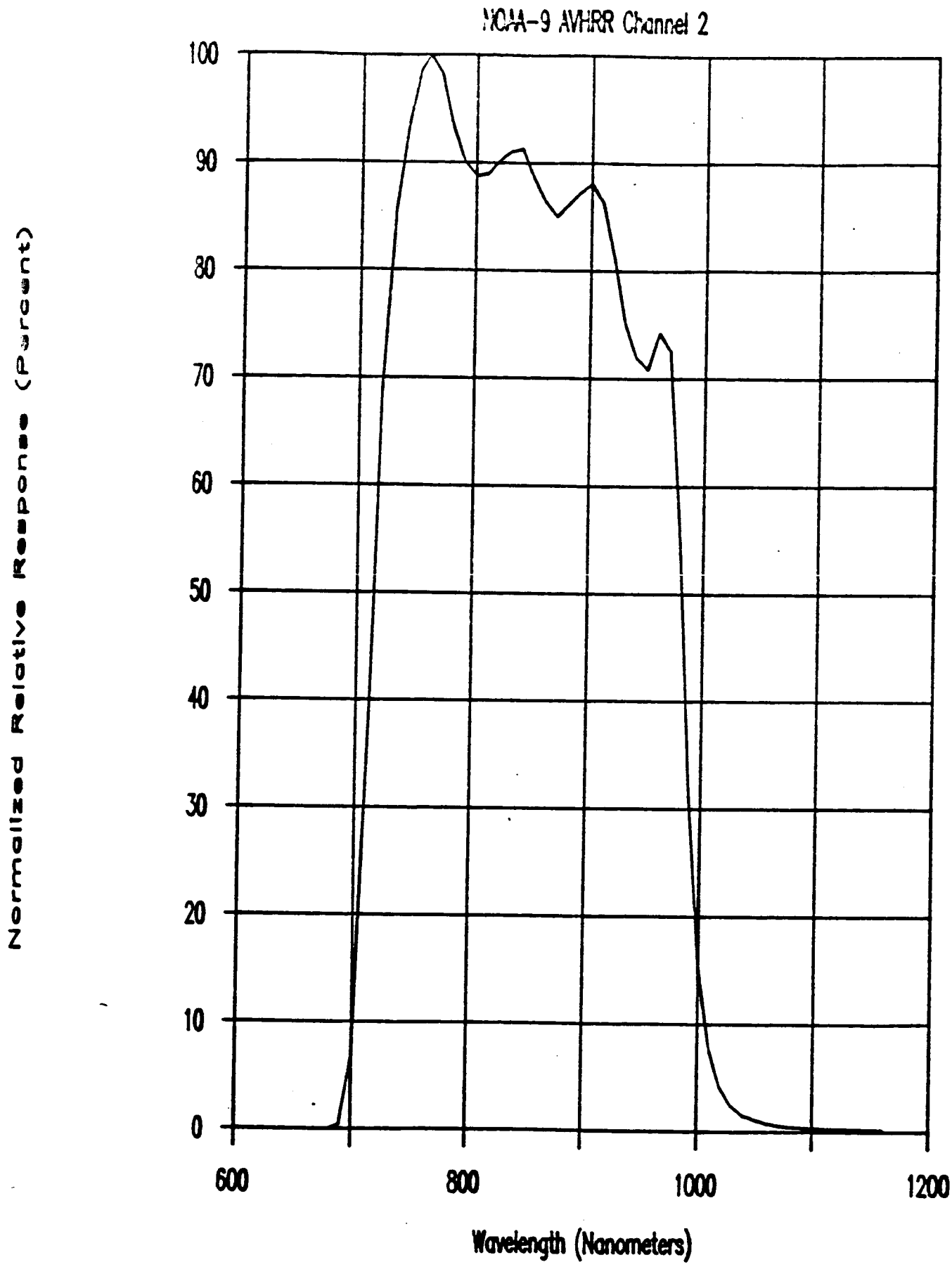

Figure 5b. Relative Spectral Response for NOAA-9 AVHRR Channel 1 (Kidwell, 1986).

2.3 Prediction of Radiance at the AVHRR Sensor

Atmospheric parameters and ground reflectances for the seven wavelengths were input to the Herman radiative transfer code. Output from the code includes radiance at the entrance aperture of the AVHRR sensor, normalized for unity exo-atmospheric solar irradiance. For use in the code, the atmosphere is divided into a sufficient number of plane-parallel layers such that changes within each layer are due only to single-scattering processes. The Gauss-Seidel iterative technique is used to solve the equation of radiative transfer. Upon convergence, all multiple scattering effects have been taken into account. Values of 5.02, 0.02, and 0.04 μm were used for the maximum and minimum radii and incremental step size, respectively, for the aerosols. A vertical aerosol distribution as measured by Elterman (1966) was assumed. The aerosols were given a refractive index of 1.54-0.01i, an average value for the region as measured by Jennings et al. (1978).

Other important inputs to the Herman code include Rayleigh, aerosol, and ozone optical depth values. The Rayleigh optical depth was determined from a knowledge of the barometric pressure and wavelength. The total optical depths were determined from the slopes of Langley plots in which the log voltages from solar radiometers were plotted against air masses. In spectral regions unaffected by absorption, the Mie optical depth at any wavelength was determined by subtracting the Rayleigh from the total optical depth at that wavelength. An optical depth versus wavelength curve was fitted through the points that spanned the absorption region due to ozone (Figure 7). The differences between the values on this curve at a given wavelength and the total minus Rayleigh value at the same wavelength gave the ozone optical depth at that wavelength. A Junge radial size distribution (Junge, 1963) was ν assumed for the aerosols. The Junge ν parameter is defined in the equation

Figure 6. Reflectance factor variations as a function of view angle for two solar zenith angles on March 15, 1986. The curves are for TM bands 1 to 4 with the bands in order starting with band 1 at the bottom in each case.

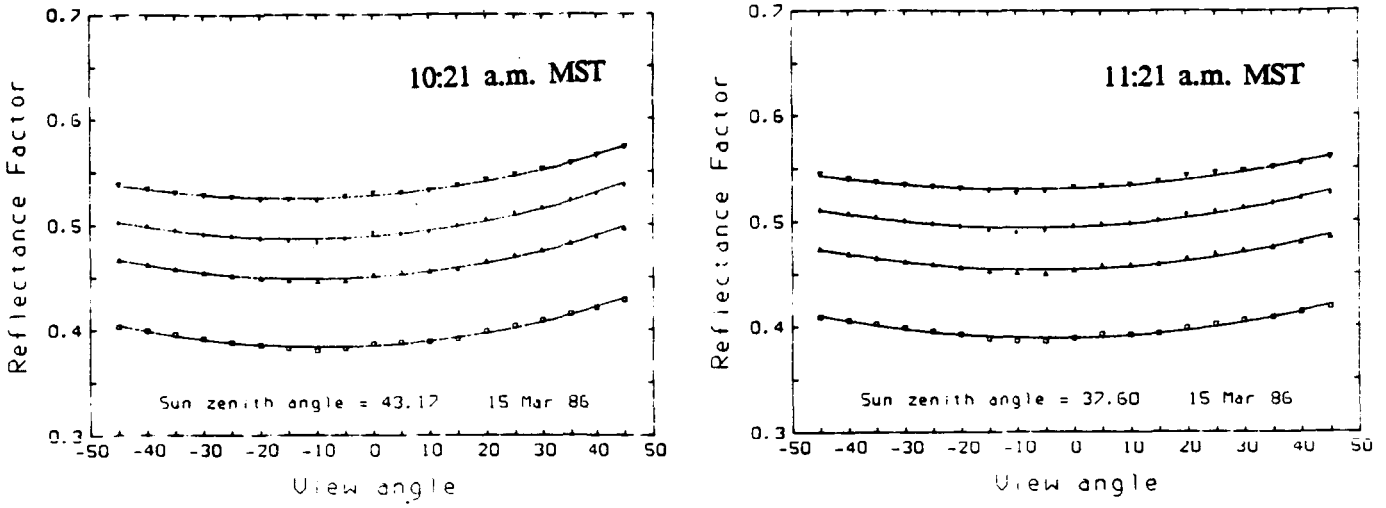

Figure 7. Optical depth versus wavelength plot used to determine ozone optical depth.

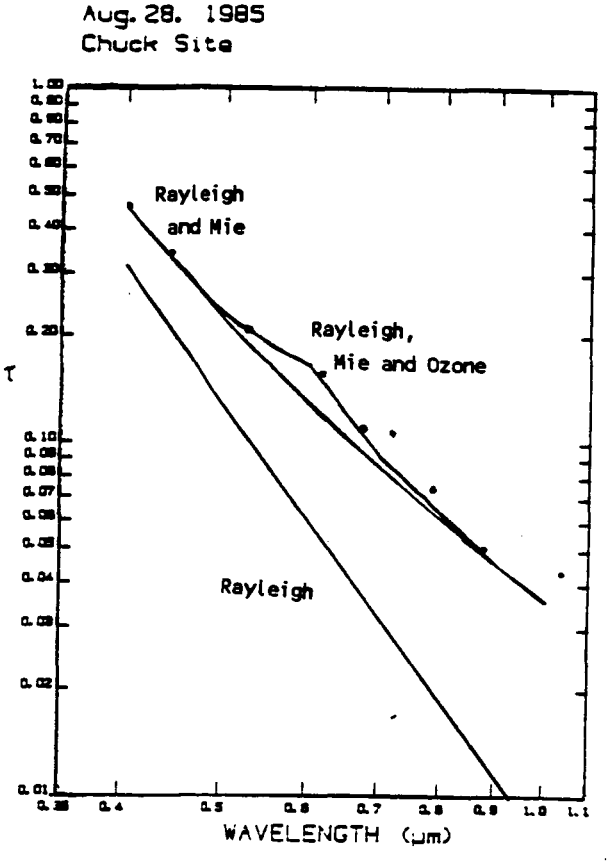

$$\frac{dN}{dr} = Cr^{-(\nu+1)}$$

where N is the number of particles, r is their radius, and C is a constant. The value of ν, needed to find the aerosol phase function, was determined from the slope of the log τ_{Mie} versus log λ curve.

The results are summarized in Tables 5 and 6. The code spectral radiance is the product of the exo-atmospheric irradiance and the normalized radiance determined from the Herman code. The exo-atmospheric solar irradiance data are those recommended by Frohlich and published by Iqbal (1983). They represent a carefully edited combination of results published by Neckel and Labs, Thekaekara, Arvesen, and others. The values were adjusted to yield an integrated value of 1367 Wm^{-2}, the solar constant as proposed by the World Radiation Center.

2.4 Reconstitution of Predicted Radiances into the AVHRR Bands

In order to combine the code spectral radiance results for the narrower bands, weighting coefficients were determined from the areas under selected intervals of the relative spectral response profiles for each AVHRR band (Figure 5). For example, the weighting coefficient for 595 nm is given by

$$\frac{\int_{530}^{610} R(\lambda)d\lambda}{\int_{530}^{800} R(\lambda)d\lambda}.$$

The code spectral radiance in each AVHRR band is then the weighted sum of code spectral radiances for the narrower bands (Tables 5 and 6). The central wavelengths listed for the AVHRR bands were calculated by the moments method (Palmer, 1984).

Table 5. Calibration of NOAA-9 AVHRR Band 1 at White Sands on August 28, 1985.

Solar Zenith Angle Z: 39.85
Solar Distance in AU: 1.0098
Junge Size Distribution: 3.77
Aerosol Size Range: 0.82 to 5.02 μm
Refractive Index: 1.54 - 0.01i
Time of Overpass: 21:27 (universal time)
Calculated Visibility: 200 km

Location: Alkali Flat
Latitude: 32 degree 47 min.
Longitude: 106 degree 22 min.
Satellite Zenith Angle: 23.62 Degree
Satellite Azimuth Angle: 255.00 Degree

Wavelength in nm	595	635	680
Bandwidth	530 - 610	610-660	660-800
Tau Mie	0.0711	0.0633	0.0561
Tau Rayleigh	0.0618	0.0474	0.0359
Tau Ozone	0.0338	0.0219	0.0102
Spectral Reflectance	0.4930	0.5110	0.5260
Exoatmospheric E0 (W/m2.μm)	1785	1630	1472.5
Normalized Code L	0.1079	0.1151	0.1220
Spectral Radiance	188.86	184.10	176.20
Weighting Coefficients	0.2912	0.3677	0.3411
Weighted Spectral Radiance	54.988	67.686	61.256

Central Wavelength for (μm):	0.6400
Code Spectral Radiance (W/m2.μm.sr):	183.94
Average Image Digital Counts (2 by 2 pixels):	367.25 (10-bit scale)
Spectral Radiance from Preflight Calibration (W/m2.μm.sr):	172.25
%(Code-Pre)/Pre:	6.78
Code Counts Per Unit Radiance:	1.9967
Preflight Counts Per Unit Radiance:	2.1321
Average Reflectance from TM3 (8/28/85):	0.5100
Apparent Reflectance R (5S):	0.4730
Spectral Radiance from 5S (L=R*cosZ*1544/3.14159 W/m2.μm.sr):	178.47
%(5S-Pre)/Pre (Radiance):	3.61
Total Gas Transmittance:	0.9400
Ozone Transmittance:	0.9550
Total Gas Transmittance Except Ozone:	0.9843
Radiance Predicted at the Sensor (Pcode):	181.04
%(Pcode-pre)/pre:	5.10
%(5S-Pcode)/Pcode:	-1.42
Counts Per Unit Radiance:	2.0285

Table 6. Calibration of NOAA-9 AVHRR Band 2 at White Sands on August 28, 1985

Solar Zenith Angle: 39.85
Solar Distance in AU: 1.0098
Junge Size Distribution: 3.77
Aerosol Size Range: 0.02 to 5.02 μm
Refractive Index: 1.54 - 0.01i
Time of Overpass: 21:27 (universal time)
Calculated Visibility: 200 km

Location: Alkali Flat
Latitude: 32 degree 37 min
Longitude: 106 degree 22 min
Satellite Zenith Angle: 23.62 Degree
Satellite Azimuth Angle: 255.00 Degree

Wavelength in nm	760	840	900	960
Bandwidth	680-800	800-870	870-950	950-1160
Tau Mie	0.0459	0.0385	0.0340	0.0304
Tau Rayleigh	0.0229	0.0153	0.0116	0.0089
Tau Ozone	0.0040	0.0016	0.0000	0.0000
Spectral Reflectance	0.5360	0.5510	0.5628	0.5710
Exoatmospheric E0 (W/m2.μm)	1222.5	1020.0	913.0	771.0
Normalized Code L	0.1265	0.1311	0.1344	0.1368
Spectral Radiance	151.71	131.15	120.37	103.41
Weighting Coefficients	0.3403	0.2601	0.2728	0.1268
Weighted Spectral Radiance	51.624	34.118	32.833	13.115

Central Wavelength (μm):	0.8460
Code Spectral Radiance (W/m2.μm.sr):	131.69
Average Image Digital Counts (2 by 2 pixels):	327.31 (10-bit scale)
Spectral Radiance from Preflight Calibration (W/m2.μm.sr):	96.633
%(Code-Pre)/Pre:	36.28
Code Counts Per Unit Radiance:	2.4855
Preflight Counts Per Unit Radiance:	3.3872
Average Reflectance from TM4 (8/28/85):	0.5550
Apparent Reflectance R (5S):	0.4660
Spectral Radiance from 5S (L=R*cosZ*999.2/3.14159 W/m2.μm.sr):	113.79
%(5S-Pre)/Pre (Radiance):	17.75
Total Gas Transmittance:	0.8490
Ozone Transmittance:	0.9980
Total Gas Transmittance Except Ozone:	0.8507
Radiance Predicted at the Sensor (Pcode):	112.03
%(Pcode-pre)/pre:	15.93
%(5S-Pcode)/Pcode:	1.57
Counts Per Unit Radiance:	2.9217

A final adjustment was applied to the code spectral radiances to correct for gaseous absorption. The Herman code takes into account ozone optical depth but does not consider H_2O, CO_2, and O_2 transmittance. In AVHRR band 2, there is significant absorption around 0.94 μm due to water-vapor and around 0.76 μm due to oxygen. Thus, the "5-S" atmospheric program of Tanre et al. (1985) was run to obtain the total gaseous transmittance due to the four gases (H_2O, O_3, CO_2, O_2). The final radiance values predicted at the AVHRR sensor are the product of total gas transmittance except ozone and the code spectral radiance (Tables 5 and 6).

2.5 Discussion of Calibration Results

Compared to the pre-launch calibration (from February, 1980) for the NOAA-9 AVHRR sensor (Smith, 1987), the results indicate response degradations of 5.1% and 15.9% in AVHRR bands 1 and 2, respectively. The outcome of this analysis differs significantly with the results of a high-altitude aircraft calibration of the NOAA-9 AVHRR carried out over White Sands on August 26, 1985 (Table 7). According to Smith et al. (1987a), the aircraft calibration results show no degradation in channel 1 and 6.3% degradation in channel 2. A more detailed analysis of the same data set (Smith et al., 1987b) indicates degradations of +2 ± 5% for channel 1 and -2 ± 5% for channel 2, i.e. no significant change. Flight data from October and November 1986 have also been analyzed (Smith et al., 1987a), indicating decreases in sensor response of 14.3% and 23.2% in AVHRR bands 1 and 2, respectively.

The work of Frouin (1987) and Frouin and Gauthier (1987) on AVHRR calibration should also be mentioned. Using standard parameters, the dunes area at White Sands and dark space digital counts, but without reference to any near-coincident ground or atmospheric measurements, they monitored the gain of several satellite sensors as a function of time. For the NOAA-9 AVHRR in the same October-November 1986 time frame studied by Smith et al. (1987a), the results from this completely different approach are quite close, with degradations of 12.9 ± 8%

for channel 1 and 23.7 ± 8% for channel 2 (Frouin, 1987). Frouin and Gauthier (1987) monitored the NOAA-7 AVHRR sensor from September 1983 to December 1984 using the same technique, encompassing the analysis of at least 100 pixels in each of twelve AVHRR scenes during that time period. Their results show no systematic changes in gain during that time, but the response degradation with respect to the pre-launch calibration (Kidwell, 1986) was 14 ± 8% for AVHRR band 1 and 15 ± 8% for band 2 (Table 7).

Table 7. Change in sensor response with time since launch (in percent), with respect to pre-launch calibration coefficients from Smith (1987) for NOAA-9, and from Kidwell (1986) for NOAA-7.

Months Since Launch	AVHRR Channel Number	NOAA-9 AVHRR[1]	NOAA-9 AVHRR[2]	NOAA-9 AVHRR[3]	NOAA-9 AVHRR[4]	NOAA-7 AVHRR[5]
8	1	- 5.1%	0%	-2 ± 5%		
	2	-15.9%	-6.3%	+2 ± 5%		
22	1		-14.3%		-12.9 ± 8%	
	2		-23.2%		-23.7 ± 8%	
28	1					-14 ± 8%
	2					-15 ± 8%
43	1					-14 ± 8%
	2					-15 ± 8%

[1] This Study
[2] Smith et al., 1987a
[3] Smith et al., 1987b
[4] Frouin, 1987
[5] Frouin & Gauthier, 1987

It is worth noting that the change between August 1985 and October/November 1986, according to Smith et al. (1987a), is considerably larger than that between launch (December, 1984) and August 1985. This trend differs from what has been observed with other sensors such as CZCS and TM, where the degradation was greatest in the months just after launch and the rate of change decreased thereafter.

The reasons for the discrepancy between our ground-based reflectance approach and NOAA's aircraft-based radiance approach for August 1985 are not known, although the two methods are completely different in almost all respects. It is hoped that the analysis of additional data sets by both groups will clarify the situation.

As a final comment in this section, Frouin (1987) has pointed out that there are several different values for the NOAA-9 AVHRR pre-launch gain coefficients available (Table 8). Thus, when monitoring and reporting changes in sensor responsivity with time, it is important to base results on a consistent set of pre-launch values.

Table 8. Various Versions of NOAA-9 AVHRR Pre-launch Gain Coefficients Expressed in Radiance ($W/m^2sr\mu m$) per unit count.

Source	NOAA-9 AVHRR Band 1	NOAA-9 AVHRR Band 2
NASA/GSFC	0.5243	0.3286
Smith (1987)	0.5246	0.3363
Kidwell (1986)	0.5191	0.3724

3.0 Current Status and Plans

The current status of the AVHRR calibration studies, including future plans, can be summarized as follows.

(1) A first pass through the analysis of the data set for August 28, 1985 has been completed. Preliminary results indicate significant degradation in the response of

both AVHRR bands 1 and 2. These results are currently in the process of being verified.

(2) Additional data sets involving AVHRR data, same-day imagery from a higher-resolution sensor, and ground measurements are being prepared (Table 9). In particular, the next data set to be analyzed consists of Landsat-5 TM and NOAA-9 AVHRR image data acquired on March 27, 1987 at White Sands together with surface reflectance and atmospheric data collected in the usual manner for Chuck Site. In general, it has not proven to be easy to obtain AVHRR and TM data sets on the same field sortie day at White Sands, with the AVHRR nadir view angle less than about 40^{0} and the weather remaining clear for both overpasses. Another problem which was not anticipated is the difficulty in obtaining archival AVHRR data. A complete archive does not exist at NASA, NOAA, Scripps or the EROS Data Center, and this has severely limited out ability to perform retrospective comparisons of AVHRR calibrations. We have also encountered problems with the reliability of data acquisitions from both TM and HRV. In the TM case it appeared to be due to a breakdown in communications between EOSAT and the Prince Albert receiving station and in the HRV case it was due to an error in the input of the sensor pointing angle. In both cases it involved the loss of potentially valuable data together with the considerable waste of time and effort of field teams numbering about ten people in each case.

(3) During the next six months, field sorties are being planned to coincide with TM and/or HRV overpasses and with same-day AVHRR overpasses for which nadir view angles do not exceed 40 degrees. It is hoped that two or three additional study cases can be acquired and analyzed for the purpose of AVHRR radiometric calibration, including the NOAA-10 AVHRR instrument.

Table 9. Status of Sensor Data Reduction (August 1987)

Date	Place	Sensor	Overpass Time (UT)	SZA	SAA	VAG	AAG	Comments
28 Aug 85	WSMR	TM (Landsat 5)	17:08:24	36	124	5.0		Preliminary
		AVHRR (NOAA 9)	21:27:00	40	242	23.6	255.0	Analysis Completed.
14 Oct 86	EAFB	AVHRR (NOAA 9)						
		AVHRR (NOAA 10)						
		AIS						
27 Mar 87	WSMR	AVHRR (NOAA 10)	15:15:45	62	107	21.5W	284.6	CCT from NOAA read.
		TM (Landsat 5)	17:01:03	43	129	0	0	CCT from EOSAT read.
28 Mar 87	WSMR	AVHRR (NOAA 10)	12:54:05	65	104	12.5E	102.4	CCT from NOAA read.
		HRV-1 (SPOT 1)	18:18:21			31.2W	278.7	DC values received from CNES.
04 May 87	EAFB	AVHRR (NOAA 9)	22:29:54	41	252	15.3E	81.7	CCT from Scripps read.
		AVIRIS						
05 May 87	EAFB	AVHRR (NOAA 9)	22:19:03	39	250	31.3E	81.7	CCT from NOAA read.
		AVIRIS						CCTs received from JPL.
		AVHRR (NOAA 10)	16:10:14	52	97	28.2W	279.4	CCTs unavailable.
17 Jul 87	WSMR	AVHRR (NOAA 10)	14:46:32	59	183	32.3E	99.2	CCT requested from EDC and Scripps.
		HRV-? (SPOT 1)	17:39:06	23	113	30.2E	99.0	DC values requested from CNES.

	Latitude	Longitude	Elevation
WSMR = White Sands Missile Range	32° 55'	106° 22'	1196 m.
EAFB = Edwards Air Force Base	35° 00'	117° 50'	694 m.

SZA = solar zenith angle
SAA = solar azimuth angle
VAG = viewing angle from ground to sensor
AAG = azimuth angle at ground

(4) Other measurement and analysis possibilities under consideration include the collection of ground-based data at Chuck Site at the time of the AVHRR overpass, and the use of the extended black lava area at White Sands in both TM and AVHRR imagery as a dark target for estimating atmospheric parameters.

(5) The current methodology makes use of the Herman code, supplemented by the "5-S" code and actual ground-based measurements of atmospheric conditions and surface reflectance, to predict spectral radiance values at the AVHRR sensor. The approach takes advantage of a reasonably precise calibration of TM image data acquired on the same day to derive an absolute calibration for the AVHRR imagery. It is of interest to learn to what extent the calibration process can be simplified, possibly even to the point where no ground measurements are required, for relative intercalibration purposes. Initially, this investigation will involve the "5-S" atmospheric code modified to give results in an inverse mode, accepting apparent reflectance at satellite altitude and computing the ground reflectance. In this way, TM imagery, assumed to be well calibrated independently, can be used with "5-S" to generate ground reflectances for the alkali-flat region of White Sands. With suitable adjustments for non-lambertian effects and wavelength dependence, these ground reflectances can then be used with "5-S" in the forward mode to predict radiances at the AVHRR sensor on the same day. It may be that the unknown atmospheric conditions will not affect the calibration significantly because of the two-way use of the "5-S" code. More specifically, the sensitivity of this procedure to uncertainties in key atmospheric parameters will be examined.

If results from this approach compare favorably with the more detailed methodology and are not overly sensitive to atmospheric conditions, the implication is that a reasonable calibration of satellite sensors with no on- board calibration capability may be possible by transfer without the necessity of making ground-based

measurements. In this way, it would be relatively straightforward to monitor occasionally the status of the AVHRR sensor's radiometric response.

4.0 Concluding Remarks

The early results of an absolute radiometric calibration of the NOAA-9 AVHRR sensor indicate significant degradations in the response of bands 1 and 2 compared to pre-launch values. The results are currently in the process of being verified and it may be that refinements of the methodology will be in order as additional data sets are analyzed. Consequently, the reported results should not be considered conclusive for the time being. Nevertheless, the Landsat TM calibration used in this approach is known to be very precise and the Herman radiative transfer code, supplemented by the "5-S" code for gaseous transmission, is reliable as well. The extent to which other steps in the analysis procedure give rise to uncertainties in the results is currently under investigation. Particular attention is being given to the geometric matching of the AVHRR and TM imagery, as well as to the spectral redistribution procedure.

By taking advantage of a reasonably precise calibration of TM imagery acquired on the same day as the AVHRR data at White Sands, a promising approach to the in-orbit calibration of AVHRR sensors is being developed. Current efforts involve primarily the examination of additional test cases and the investigation of possible simplifications in the procedure through judicious use of atmospheric models.

5.0 Acknowledgements

We wish to thank the staffs at EOSAT and SPOT Image for their interest and close collaboration in this work. We also wish to thank Robert Frouin (Scripps), Brian Markham (NASA/GSFC) and Gilbert Smith (NOAA) for their help in searching for AVHRR data for our retrospective analysis. Finally, we wish to thank Gilbert Smith and Robert Frouin for the benefit of several discussions of their results.

6.0 References

Elterman, L. (1966), Aerosol measurements in the troposphere and stratosphere, Appl. Opt., 5:1769-1776.

Frouin, R. (1987), communication to the authors.

Frouin, R., and Gauthier, C. (1987),Calibration and NOAA-7 AVHRR, GOES-5, and GOES-6 VISSR/VAS solar channels, Remote Sens. Environ., 22:73-101.

Herman, B. M., and Browning, S. R. (1975), The effect of aerosols on the earth-atmosphere albedo, J. Atmos. Sci., 22:158-165.

Iqbal, M. (1983), An Introduction to Solar Radiation, Academic, New York.

Jackson, R. D., Moran, M. S., Slater, P. N., and Biggar, S. F. (1987), Field calibration of reference reflectance panels, Remote Sens. Environ., 22:145-158.

Jennings, S. G., Pinnick, R. G., and Auvermann, H. J. (1978), Effects of particular complex refractive index and particle size distribution variations on atmospheric extinction and absorption for visible through middle IR wavelengths, Appl. Opt., 17:3922-3929.

Junge, C. E. (1963), Air Chemistry and Radioactivity, Academic, New York.

Kidwell, K. B. (1986), NOAA polar orbiter data (TIROS-N, NOAA-6, NOAA-7, NOAA-8, NOAA-9 and NOAA-10) users guide, Satellite Data Service Division, National Climatic Data Center, NOAA/NESDIS, U. S. Department of Commerce, Washington, D.C.

Palmer, J. M. (1984), Effective bandwidths for Landsat-4 and Landsat D' Multispectral Scanner and Thematic Mapper subsystem, IEEE Trans. Geosci., Remote Sens., GE-22:336-338.

Robinson, B. F., Bauer, M. E., Dewitt, D. P., Silva, L. F., and Vanderbilt, V. C. (1979), Multiband radiometer for field research, SPIE 196:8-15.

Slater, P. N., Biggar, S. F., Holm, R. G., Jackson, R. D., Mao, Y., Moran, M. S., Palmer, J. M. and Yuan, B. (1987), Reflectance- and radiance-based methods for the in-flight absolute calibration of multispectral sensors, Remote Sens. Environ., 22:11-37.

Slater, P. N., Biggar, S. F., Holm, R. G., Jackson, R. D., Mao, Y., Moran, M. S., Palmer, J. M., and Yuan, B. (1986), Absolute radiometric calibration of the Thematic Mapper, SPIE 660:2-8.

Smith, G. R. (1987), communication to the authors.

Smith, G. R., Levin, R. H., and Koyanagi, R. S., (1987a), Calibration of the solar channels of the NOAA-9 AVHRR using high altitude aircraft measurements, preprint.

Smith, G. R., Levin, R. H., Abel, P., and Jacobowitz, H (1987b), Calibration of the solar channels of the NOAA-9 AVHRR using high altitude aircraft measurements, preprint.

Tanre, D., Deroo, C., Dahaut, P., Herman, M., Mocrette, J. J. Perbos, J., and Deschamps, P. Y. (1985), Effets atmospheriques en teledetection-logiciel de simulation du signal satellitaire dans le spectre solaire, Proc. Third Int. Colloq. on Spectral Signatures of Objects in Remote Sensing, ESA SP-247, pp. 315-319.